Journal of Chemical and Petroleum Engineering (JChPE)

Print ISSN: 2423-673X Online ISSN: 2423-6721

Physical/Rheological Characteristics of Bitumen Modified by SBS, ZnO, TiO_2 and EVA Precursors

Fariba Karimian , Younes Beygi-Khosrowshahi *

1. Department of Chemical Engineering, Islamic Azad University of Ilkhchi Branch, Tabriz, Iran. E-mail: f_karimiankh@yahoo.com
2. Department of Chemical Engineering, Faculty of Engineering, Azarbaijan Shahid Madani University, Tabriz, Iran. y.beygi@azaruniv.ac.ir

ARTICLE INFO

Article History:
Received: 31 August 2020
Revised: 27 April 2021
Accepted: 28 April 2021

Article type: Research

Keywords:
EVA,
Modified Bitumen,
SBS,
TiO_2,
ZnO

ABSTRACT

Owing to climate conditions, heavy traffic loads, and increasing axial loads, conventional bitumen/asphalt should be modified. Bituminous materials are also vulnerable to aging during pavement construction and service time, which will seriously affect bitumen pavement's service performance/life. To this end, bitumen was modified using styrene-butadiene-styrene (SBS), ZnO, TiO_2 and ethylene vinyl acetate (EVA). The applied methodology was Mixture Design The contents of SBS, ZnO, TiO2 and EVA were considered independent variables. Response variables followed as: G*/sin OB, G*/sin RTFO, G*/sin PAV, RV, penetration (PEN), softening, ductility, m-value and stiffness. Results of experiments of penetration degree, softening point, and ductility performed on basic bitumen without any additives were 89, 49 °C, and 137, respectively. Effects of independent variables were investigated on response variables using mathematic models and optimized compositions. SBS, ZnO, TiO_2, and EVA precursors positively affected the PEN parameter. Manipulated samples possessed a penetration range of 48–62 (1/10 mm). Maximum softening was reached at the highest EVA, and the minimum softening was detected at the largest ZnO and TiO_2. Softening point ranged in 59–71 °C. SBS, ZnO, TiO_2, and EVA components positively increased ductility, and the largest positive effect belonged to SBS. SBS and EVA positively affected G^*/sin OB response, whereas ZnO and TiO_2 variables negatively decreased it. Dynamic shear rheometric (DSR) data for aged bitumens within short-term periods decreased from 52 to 76 °C for all investigated samples. All mentioned modifications were performed to optimize the performance of ultimate bitumen from perspectives of softening, ductility, strength, m-value, stiffness, etc.

Introduction

Bituminous materials are vulnerable to aging during the construction and service time of pavement, which will seriously affect the service performance/life of bitumen pavement [1, 2]. According to different stages during the construction and application of asphalt pavement, the aging is divided into short-term and long-term aging. Short-term aging occurs in the mixing, transportation, paving and compaction of bituminous mixture [3]. The short-term aging is usually simulated by TFOT or rolling thin film oven test (RTFOT). In addition, long-term aging happens during the service time of pavement. Based on different causes of bitumen aging, long-

* Corresponding Author: Y. Beygi-Khosrowshahi (E-mail address: y.beygi@azaruniv.ac.ir)

Journal of Chemical and Petroleum Engineering, 2021, 55(2): 189- 202.
Publisher: University of Tehran, College of Engineering *DOI: 10.22059/jchpe.2021.309128.1329*

term aging is further categorized into long-term thermal oxidation aging and long-term photo-oxidation aging [4–6]. The PAV is also used to simulate long-term thermal oxidation aging, while UV radiation is used to simulate long-termphoto-oxidation aging. In order to enhance the aging resistance of bitumen, many studies have been conducted. Generally, adding anti-aging modifiers to bitumen for enhancing the aging resistance is the main method. The anti-aging modifiers mainly include antioxidant [7–9], UV absorber [9–12], layered silicates [12–15], and inorganic nanoparticles [16–20]. Recently, the effects of nano-zinc oxide and organically expanded vermiculite were investigated on the rheological characteristics of different bitumens before and after aging [21].

Recent decades, bitumen's properties have been modified with various additive materials [22]. By large, the polymeric additives have been utilized in the bitumen modification. The styrene-butadiene-styrene (SBS) block copolymers are widely used to elevate the resistance of mixtures against to rutting and fatigue at high temperatures [23–26]. However, the increased content of SBS caused worsening of the low service temperature [27]. A created rubbery network improves the elastic response and enhances the low temperature cracking resistance in case the SBS-rich phase forms [28]. Many researchers have focused on the improvement of service life of asphalt pavement against vehicles dynamic loads by using of nanomaterials such as TiO_2, SiO_2, nanoclay [29–34]. Shafabakhsh et al. [35] evaluated the influence of nano-TiO_2 on the engineering properties of bitumen and asphalt concrete mixtures. Micromechanical modeling of shear modulus of crumb rubber modified bitumen was performed by Wang et al. [36]. Daryaee et al. [37] applied the waste polymer modified bitumen with rejuvenator in high reclaimed asphalt pavement mixtures. The effect of different fillers was also investigated on the SBS modified bitumen aging [38]. In another research, the physical, chemical and morphology characterization of nanoceramic powder was probed as a bitumen modification [39].

Mixture design A, type D-Optimal was utilized in this research and the values of SBS, ZnO, TiO_2, and EVA were considered as the independent variables. The dependent or response variables followed as G*/sin OB, G*/sin RTFO, G*/sin PAV, RV, PEN, soft, ductility, m-value, and stiffness. The effects of independent variables were investigated on the response variables using the mathematic models and the optimized compositions. All the mentioned modifications were carried out to optimize the performance of ultimate bitumen from the perspectives of softening, ductility, strength, m-value, stiffness, etc. Instead of doing some costly and time-consuming empirical activities, the methodology introduced in the current work can easily optimize the bitumen features and predict its behavior. That is to say, the optimization details are going to be released in a parallel work, which is underway.

Materials and Methods

The utilized materials in the current work, including the SBS (GF00679361), ZnO (544906), TiO_2 (637254), and ethylene vinyl acetate (EVA; 181080), were purchased from Sigma-Aldrich and used without any purification. The methodology of Mixture design A, type D-optimal was employed in the current work, and the values of SBS, ZnO, TiO_2, and EVA were considered as the independent variables. The design matrix with a total of 19 runs was generated using Design-Expert 7.0.0 software. Each design was evaluated separately, based on the influence of each component of variables towards the response. The composition of each run was conducted in a randomized order, according to the D-optimal model design to minimize the effect of unexplained variability on the actual response, owing to the extraneous factor. Table 1 reports the amounts of independent variables applied in the designed experiments. In the first stage, the blends were produced in the laboratory using a shear mixer, according to Table 1. The neat bitumen the prepared blends, were then characterized by the tests of dynamic shear rheometer (DSR), etc.

Table 1. The applied amounts of independent variables in the designed experiments.

Component	Unit	Name	Type	Low	High
A	%	TiO_2	Mixture	0	2
B	%	ZnO	Mixture	0	2
C	%	SBS	Mixture	0	5
D	%	EVA	Mixture	0	5

Results and Discussion

Penetration Experiments

The penetration degrees of different samples of X_1, X_2, X_3… X_{20} are tabulated in Table 2. The results of variance analysis for the penetration (PEN) response are tabulated in Table 2. The results of experiments of penetration degree, softening point, and ductility performed on the basic bitumen without any additives were 89, 49 °C, and 137, respectively. The linear model was adopted to predict the influence of compositions of SBS, ZnO, TiO_2, and EVA for the penetration. The variance analysis demonstrated that the p-value was meaningful for the selected model. These results with a high R-Squared coefficient (= 0.997) and a high adequacy precision (= 141.43) approved the accuracy of the used model. Furthermore, the variance analysis depicted the meaningful effects of the linear mixture of SBS, ZnO, TiO_2, and EVA variables on the PEN responses (p-value < 0.0001), and the linear model opted for the PEN response as follows:

$$
\begin{aligned}
\text{PEN}= \quad & +9.33063 \quad * \text{TIO2} \\
& +10.97345 \quad * \text{ZNO} \\
& +7.11054 \quad * \text{SBS} \\
& +6.19198 \quad * \text{EVA}
\end{aligned}
$$

An investigation conducted on the linear coefficients displayed that the SBS, ZnO, TiO_2, and EVA precursors positively affected the PEN parameter. The highest positive coefficient or the lowest influence on the decrement of PEN degree was associated with the ZnO, and the lowest positive coefficient or the highest impact on the decrease of PEN degree was correlated with the EVA-based systems.

Table 2. Results of variance analysis for the PEN response

Source	Sum of Squares	df	Mean Square	F Value	p-value Prob > F	
Model	387.83	3	129.28	1841.6	< 0.0001	significant
Linear Mixture	387.83	3	129.28	1841.6	< 0.0001	
Residual	1.12	16	0.07			
Lack of Fit	0.62	11	0.057	0.57	0.7993	not significant
Pure Error	0.5	5	0.1			
Cor Total	388.95	19				
R^2= 0.997						
Adeq Precision = 141.43						

Fig. 1 also exhibits the three-dimensional (3D) graph for the effect of variables designated with A= TiO_2, B = ZnO, and D = EVA (with the constant SBS content at the level of 2.5%) for the PEN response. The largest PEN was detected at the maximum levels of ZnO and TiO_2, whereas the smallest PEN was observed at the maximum level of EVA precursor.

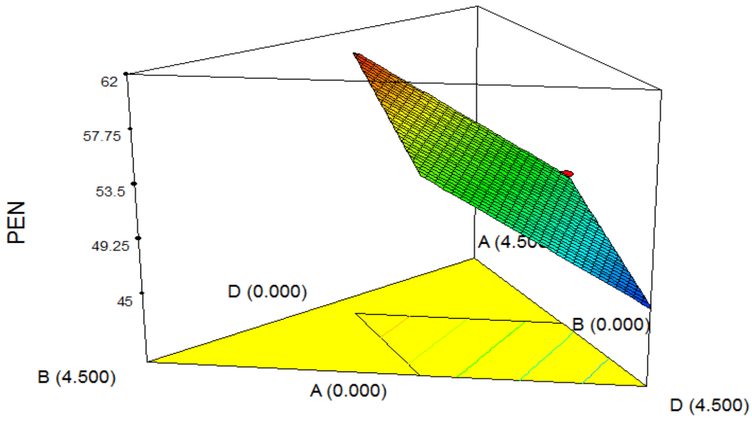

Fig. 1. 3D plot for the effect of variables designated by A= TiO_2, B = ZnO, and D = EVA on the PEN degree

Softening Point Experiments

The results recorded for the softening points of all samples (X_1, X_2, X_3… X_{20}) are tabulated in Table 3. Table 3 also collects the data reached from the variance analysis for the softening response. Softening point also ranged from 59–71 °C. A linear model is selected to predict compositional impacts of SBS, ZnO, TiO_2, and EVA on the softening point. The variance analysis manifested that the p-value was meaningful for the selected model. These data with the high R-Squared coefficient (= 0.970) and a high Adequacy Precision (= 38.60) validated the selected model to predict results. In addition, the variance analysis represented that the Linear Mixture of SBS, ZnO, TiO_2, and EVA variables had a proper influence on the softening response (p-value < 0.0001) and the mentioned linear model as follows:

Soft = +6.66211 * TIO2
+7.72335 * ZNO
+10.08329 * SBS
+10.08960 * EVA

The linear coefficient studies reflected that SBS, ZnO, TiO_2, and EVA had a positive effect on the softening. The highest positive coefficient were associated with the EVA, and the lowest was attributed to the TiO_2 precursor (Table 3).

Table 3. Results of variance analysis for the softening response

Source	Sum of Squares	df	Mean Square	F Value	p-value Prob > F	
Model	231.33	3	77.11	170.9	< 0.0001	significant
Linear Mixture	231.33	3	77.11	170.9	< 0.0001	
Residual	7.22	16	0.45			
Lack of Fit	2.72	11	0.25	0.27	0.9655	not significant
Pure Error	4.5	5	0.9			
Cor Total	238.55	19				
R^2= 0.97						
Adeq Precision = 38.6						

Fig. 2 demonstrates the 3D graph for the influences of A= TiO_2, B = ZnO, and D = EVA variables (with a constant content of SBS at the level of 2.5%) versus the softening response. It could be observed, the maximum softening was reached at the highest level of EVA, and the minimum softening was detected at the highest levels of ZnO and TiO_2.

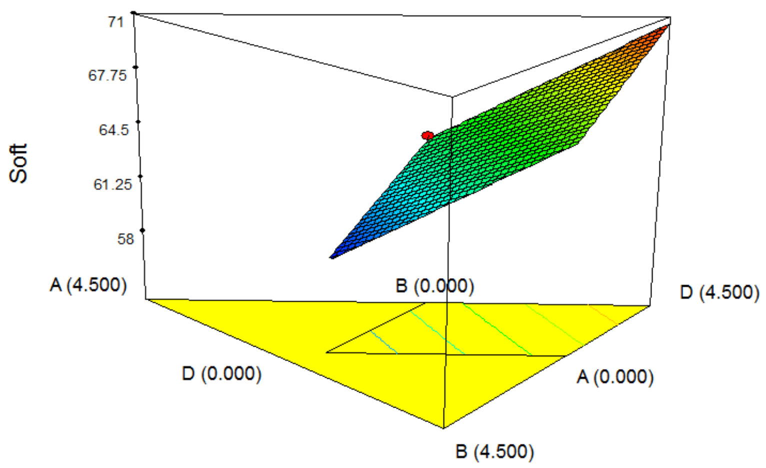

Fig. 2. 3D graph illustrating the effects of A= TiO_2, B = ZnO, and D = EVA variables on the softening point

Ductility Experiments on the Bitumen

Ductility is defined as the ability of a material to deform plastically before fracturing. The results of ductility experiment on various samples (X_1, X_2, X_3… X_{20}) are tabulated in Table 4. Likewise, Table 4 represents the results of variance analysis for the ductility response. A nonlinear quadratic model was selected for predicting the impact of composites of SBS, ZnO, TiO_2, and EVA on ductility. The variance analysis approved the validity of the selected model for the mentioned systems. The acquired data with possessing the high R-Squared coefficient (= 0.999) and the sufficient Adequacy Precision (= 227.80) validated the opted quadratic model for predicting the results. According to the variance analysis, the Linear Mixture effects of SBS, ZnO, TiO_2, and EVA were positive on the ductility response. The mutual influences of AB, AC, AD, and CD on the ductility response were also meaningful, whereas BC and BD were meaningless. The non-linear quadratic model selected for the ductility response as follows:

$$
\begin{aligned}
\text{Ductility} = \; & -4.07824 && * \text{TIO2} \\
& +5.86877 && * \text{ZNO} \\
& +10.94285 && * \text{SBS} \\
& +2.76092 && * \text{EVA} \\
& +4.28912 && * \text{TIO2} * \text{ZNO} \\
& +1.41678 && * \text{TIO2} * \text{SBS} \\
& +1.44974 && * \text{TIO2} * \text{EVA} \\
& +0.34712 && * \text{ZNO} * \text{SBS} \\
& +0.35872 && * \text{ZNO} * \text{EVA} \\
& -0.69465 && * \text{SBS} * \text{EVA}
\end{aligned}
$$

Through focusing on the coefficients, it was comprehended that the SBS, ZnO, TiO_2, and EVA components positively increased the ductility and the largest positive effect belonged to the SBS constituent. In contrast, TiO_2 negatively decreased the ductility. Furthermore, only the coefficient of mutual influence was negative for the SBS and EVA constituents.

Table 4. Data recorded from the variance analysis for the ductility response

Source	Sum of Squares	df	Mean Square	F Value	p-value Prob > F	
Model	4607.595	9	511.9550055	5361.065561	< 0.0001	significant
Linear Mixture	4547.235	3	1515.745075	15872.50566	< 0.0001	
AB	35.29023	1	35.29022707	369.5504857	< 0.0001	
AC	4.346126	1	4.34612587	45.51154979	< 0.0001	

AD	4.620556	1	4.620555529	48.38530896	< 0.0001	
BC	0.218746	1	0.218746065	2.290654415	0.1611	
BD	0.236578	1	0.236577783	2.477383737	0.1466	
CD	38.42819	1	38.42818922	402.4104454	< 0.0001	
Residual	0.95495	10	0.095495009			
Lack of Fit	0.45495	5	0.090990019	0.909900186	0.5400	not significant
Pure Error	0.5	5	0.1			
Cor Total	4608.55	19				
R^2= 0.999						
Adeq Precision = 227.80						

The 3D plot showing the influences of A= TiO_2, B = ZnO, and C = SBS variables (with a constant content of D = EVA at 2.5%) on the ductility response is represented in Fig. 3. The maximum ductility was detected at the highest levels of SBS and ZnO, while the minimum ductility was reached at the highest level of TiO_2.

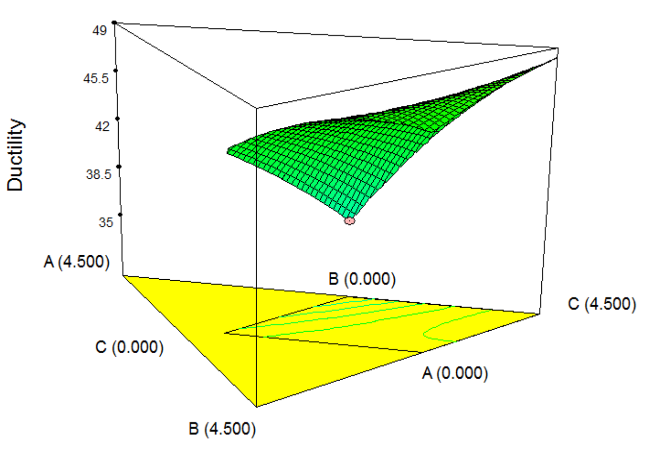

Fig. 3. 3D plot displaying the influences of A= TiO_2, B = ZnO, and C = SBS parameters on the ductility of bitumen

Viscosity Experiments (RV)

The viscosity data for all prepared samples (X_1, X_2, X_3… X_{20}) are tabulated in Table 5. The results of variance analysis for the RV response are reported in Table 5. A linear model was selected to predict the compositional influence of the SBS, ZnO, TiO_2 and EVA. Based on variance analysis, the p-value was meaningful for the opted model. The results, by owing the high R-Squared coefficient (= 0.965) and the proper Adequacy Precision (= 40.494), validated the selected model to predict results. In addition, the impacts of Linear Mixture coefficients of SBS, ZnO, TiO_2, and EVA variables on the RV responses were meaningful (p-value < 0.0001), and the selected linear model as follows:

$$
\begin{aligned}
RV = \quad & -33.59335 \quad * \text{TIO2} \\
& -48.83047 \quad * \text{ZNO} \\
& +267.19168 \quad * \text{SBS} \\
& +339.69899 \quad * \text{EVA}
\end{aligned}
$$

The investigation of the effects of independent variables utilizing a linear model represented that the SBS and EVA variables positively enhanced the RV response, in which the largest positive coefficient belonged to the EVA precursor. On the other hand, the ZnO and TiO_2 variables negatively decreased the RV response, in which the largest negative coefficient belonged to the ZnO constituent.

Table 5. Variance analysis for the RV response

Source	Sum of Squares	df	Mean Square	F Value	p-value Prob > F	
Model	3.42E+06	3	1.14E+06	146.79	< 0.0001	significant
Linear Mixture	3.42E+06	3	1.14E+06	146.79	< 0.0001	
Residual	1.24E+05	16	7768.31			
Lack of Fit	1.07E+05	11	9687.49	2.73	0.1386	not significant
Pure Error	17730.5	5	3546.1			
Cor Total	3.55E+06	19				
R^2= 0.965						
Adeq Precision = 40.494						

Fig. 4 depicts the 3D plot for shedding light on the effects of A= TiO_2, B = ZnO, and D = EVA variables (at a constant level of SBS at 2.5%) on the RV responses. The highest RV value was observed at the maximum level of EVA. On the other hand, its lowest amount was matched with the maximum levels of ZnO and TiO_2.

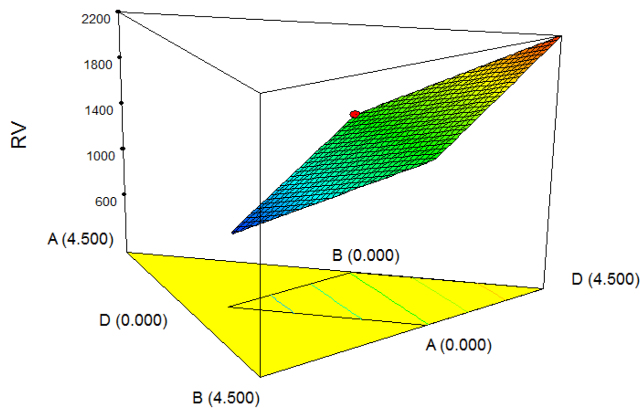

Fig. 4. 3D plot for showing the effects of A= TiO_2, B = ZnO, and D = EVA variables on the viscosity

Dynamic Shear Rheometric (DSR) Measurements

Influence of high temperatures on the unaged bitumen (OB)

The results of G^*/sin for the unaged materials at high temperatures (X_1, X_2, X_3… X_{20}) are tabulated in Table 6. The data obtained from the variance analysis for the G^*/sin OB response at 64 °C are also reported in Table 7. A linear model was also selected for predicting the compositional effects of SBS, ZnO, TiO_2, and EVA on the G^*/sin OB. The p-values were meaningful for the utilized model. The recorded data with the large R-squared coefficient (= 0.978) and the suitable Adequacy Precision (= 50.96) validated the opted model for predicting the results. Moreover, the Linear Mixture effects of SBS, ZnO, TiO_2, and EVA variables were meaningful on the G^*/sin OB responses (p-value < 0.0001), and the linear model in question was selected for the G^*/sin OB response as follows:

G*/sin OB =	-0.16333	* TIO2
	-0.51086	* ZNO
	+1.21827	* SBS
	+1.53527	* EVA

Furthermore, the dynamic shear rheometric (DSR) data for the aged bitumens within short-term periods decreased from 52 to 76 °C for all investigated samples. The investigation of the effects of independent variables by the linear model demonstrated that the SBS and EVA variables positively elevated the G^*/sin OB response. The highest positive coefficient belonged to the EVA component. In contrast, the ZnO and TiO_2 variables negatively decreased the G^*/sin OB response, in which the largest negative coefficient belonged to the ZnO constituent.

Table 6. DSR data obtained for the OB samples.

BITUMEN TYPE	OB (G*/sin α)				
	52 °C	**58 °C**	**64 °C**	**70 °C**	**76 °C**
X1	11.70	5.21	2.87	1.33	0.71
X2	18.14	9.92	4.74	2.14	0.98
X3	44.91	21.80	11.15	5.70	2.76
X4	11.59	5.81	3.22	1.45	0.83
X5	11.70	5.21	2.32	1.33	0.71
X6	23.97	11.80	5.66	3.53	1.78
X7	16.02	8.10	6.53	2.04	0.99
X8	18.14	9.92	4.26	2.14	0.98
X9	23.80	14.20	7.57	3.21	1.55
X10	22.74	11.10	6.49	3.19	1.30
X11	20.83	10.20	5.00	2.59	1.27
X12	11.59	5.81	3.22	1.45	0.83
X13	21.76	10.90	6.82	2.82	1.38
X14	23.70	11.60	7.15	3.45	1.60
X15	24.39	12.10	6.41	4.05	2.18
X16	13.75	6.40	5.70	2.10	0.91
X17	22.74	11.10	6.49	3.19	1.30
X18	28.65	14.80	6.29	3.79	1.94
X19	20.83	10.20	5.00	2.59	1.27
X20	42.37	20.4	8.94	4.95	2.31

Table 7. Variance analysis results for the DSR response of OB

Source	**Sum of Squares**	**df**	**Mean Square**	**F Value**	**p-value Prob > F**	
Model	83.50938	3	27.83646	237.2497	< 0.0001	significant
Linear Mixture	83.50938	3	27.83646	237.2497	< 0.0001	
Residual	1.877277	16	0.11733			
Lack of Fit	1.610827	11	0.146439	2.747961	0.1372	not significant
Pure Error	0.26645	5	0.05329			
Cor Total	85.38666	19				
R^2= 0.978						
Adeq Precision = 50.96						

The 3D graph for depicting the influence of A= TiO_2, B = ZnO, and D = EVA variables (at a constant level of SBS at 2.5%) on the G^*/sin OB response is reported in Fig. 5. The highest G^*/sin OB was detected at the maximum level of EVA, and the lowest G^*/sin OB was reached at the maximum level of ZnO.

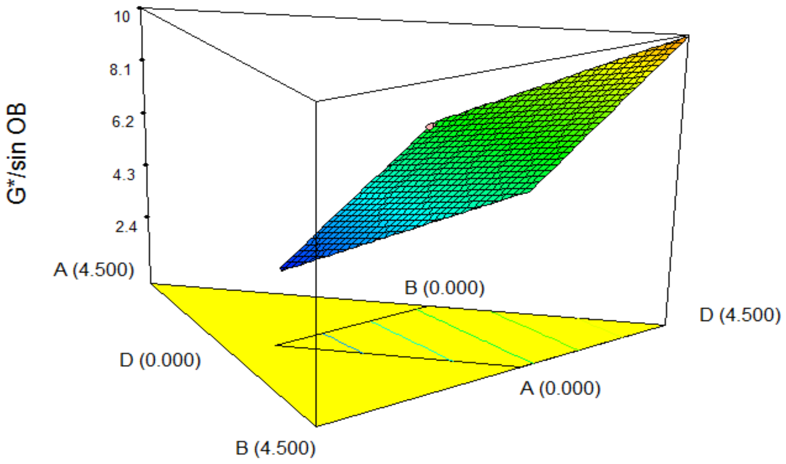

Fig. 5. 3D plot for the impacts of A= TiO_2, B = ZnO, and D = EVA variables on the G^*/sin OB response

Results of High Temperature on the Aged Bitumens in Short Periods (RTFO)

The G*/sin results for all samples aged at high temperatures within the short term periods (X_1, X_2, X_3… X_{20}) are tabulated in Table 8.

Table 8. DSR data for the aged bitumens within short term periods

BITUMEN TYPE	RTFO (G*/sin α)				
	52 °C	**58 °C**	**64 °C**	**70 °C**	**76 °C**
X1	24.70	12.61	6.48	2.99	1.53
X2	43.97	22.49	12.09	4.95	2.71
X3	71.86	35.40	19.11	8.82	4.37
X4	39.81	19.40	10.14	4.50	2.39
X5	24.70	12.61	7.54	2.99	1.53
X6	52.18	25.70	11.55	6.51	3.18
X7	41.86	20.74	10.89	4.60	2.45
X8	43.97	22.49	10.06	4.95	2.71
X9	54.05	26.67	15.25	7.14	3.26
X10	45.98	24.61	13.95	5.86	2.94
X11	44.19	23.70	11.43	5.60	2.83
X12	39.81	19.40	9.29	4.50	2.39
X13	48.69	24.80	13.65	5.97	2.99
X14	51.32	25.40	13.71	6.27	3.03
X15	56.14	27.30	13.39	8.09	4.11
X16	29.35	14.20	12.55	3.94	1.87
X17	25.98	24.61	13.96	5.86	2.94
X18	57.39	28.35	12.71	8.67	4.39
X19	44.19	23.70	11.2	5.60	2.83
X20	61.21	30.36	16.45	9.17	5.03

Table 9 also reports the results of variance analysis for the G^*/sin RTFO response at 64 °C. A linear model was similarly selected to predict compositional impacts of SBS, ZnO, TiO_2, and EVA variables on the G^*/sin RTFO. The variance analysis represented that the p-value was meaningful for the selected model. The large R-squared coefficient equal to 0.926 and the high Adequacy Precision of 27.73 validated the opted linear model for the data prediction. According to the variance analysis, the Linear Mixture influences of SBS, ZnO, TiO_2, and EVA variables were meaningful on the G^*/sin RTFO response (p-value < 0.0001) and the linear model utilized for the G^*/sin RTFO response as follows:

G*/sin RTFO = +0.27853 * TIO2
+0.20517 * ZNO
+2.14259 * SBS
+2.76385 * EVA

The linear coefficients demonstrated that the SBS, ZnO, TiO_2, and EVA all positively increased the G^*/sin RTFO. The largest positive coefficient belonged to the EVA precursors, and the smallest coefficient was for the ZnO constituent.

Table 9. Data obtained from the variance analysis for the DSR response of RTFO samples

Source	Sum of Squares	df	Mean Square	F Value	p-value Prob > F	
Model	150.8975	3	50.2991826	67.471	< 0.0001	significant
Linear Mixture	150.8975	3	50.2991826	67.471	< 0.0001	
Residual	11.92785	16	0.74549077			
Lack of Fit	8.917852	11	0.81071385	1.3467	0.3923	not significant
Pure Error	3.01	5	0.602			
Cor Total	162.8254	19				
R^2 = 0.926						
Adeq Precision = 27.73						

Fig. 6 also illustrates the 3D graph for elucidating the effects of A= TiO_2, B = ZnO, and D = EVA variables (with a constant level of SBS at 2.5%) for the G^*/sin RTFO response. The highest G^*/sin RTFO value was detected at the maximum level of EVA and conversely, the lowest G^*/sin RTFO value was acquired at the maximum levels of ZnO and TiO_2 components.

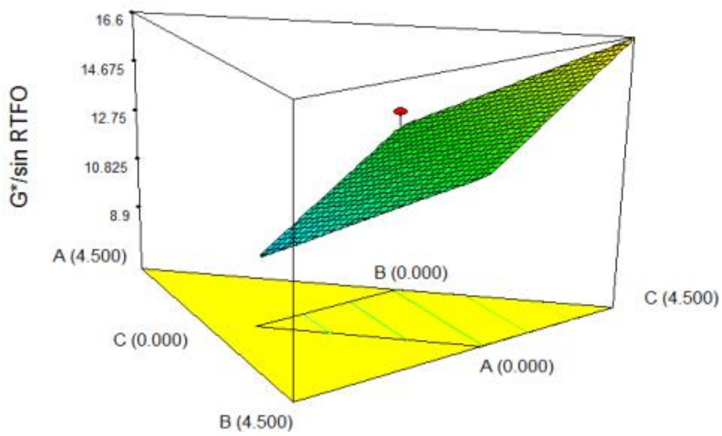

Fig. 6. 3D plot depicting the impacts of A= TiO_2, B = ZnO, and D = EVA variables on the G^*/sin RTFO response

Results of Moderate Temperatures on the Aged Bitumens within Long Terms (PAV)

The data recorded for the G^*/sin response from different aged bitumen at moderate temperatures (X_1, X_2, X_3… X_{20}) are tabulated in Table 10.

Table 10. DSR results for the PAV samples

BITUMEN TYPE	PAV (G*.sin α)		
	22 °C	25 °C	28 °C
X1	2927	2220	1790
X2	3615	3590	3080
X3	5542	5270	4850
X4	3176	2880	2380
X5	2927	2220	1790
X6	4084	4170	3810
X7	4449	3420	2900
X8	3880	3590	3080
X9	4890	4650	4190
X10	4386	3920	3640
X11	3971	3650	3210
X12	3176	2880	2380
X13	4442	3870	3500
X14	4498	4090	3770
X15	4291	4360	3950
X16	4131	3140	2690
X17	4386	3920	3640
X18	4310	4790	4450
X19	3971	3650	3210
X20	5293	5000	4620

The results of variance analysis for the G^*/sin PAV responses at 22 °C are tabulated in Table 11. A linear model was utilized to predict the compositional impacts of SBS, ZnO, TiO_2, and EVA variables on the G^*/sin PAV. The p-value was meaningful for the selected linear model. Thanks to the high R-Squared coefficient (= 0.992) and the suitable Adequacy Precision (= 87.93) values, the opted linear model was validated to predict desired results. In addition, the Linear Mixture coefficients of SBS, ZnO, TiO_2, and EVA variables represented a meaningful influence on the G^*/sin PAV response (p-value < 0.0001) and the selected linear model as follows:

$$
\begin{aligned}
G^*/\sin PAV = \quad & +206.96945 \quad * \text{TIO2} \\
& +167.37541 \quad * \text{ZNO} \\
& +733.64590 \quad * \text{SBS} \\
& +816.28285 \quad * \text{EVA}
\end{aligned}
$$

The linear coefficients approved that the SBS, ZnO, TiO_2, and EVA precursors positively affected the G^*/sin PAV. The largest positive and the smallest positive coefficients belonged to the EVA and ZnO constituents, respectively.

Table 11. Data of variance analysis for the DSR response of PAV samples

Source	Sum of Squares	df	Mean Square	F Value	p-value Prob > F	
Model	9.47E+06	3	3.16E+06	722.66	< 0.0001	significant
Linear Mixture	9.47E+06	3	3.16E+06	722.66	< 0.0001	
Residual	69887.92	16	4367.99			
Lack of Fit	34775.42	11	3161.4	0.45	0.8746	not significant
Pure Error	35112.5	5	7022.5			
Cor Total	9.54E+06	19				
R^2= 0.992						
Adeq Precision = 87.93						

The 3D plot displaying the effects of A= TiO_2, B = ZnO, and D = EVA variables (with a constant level of SBS at 2.5%) on the G^*/sin PAV response is reported in Fig. 7. The maximum

G^*/sin PAV value was attained at the highest level of EVA, and the corresponding minimum value was detected at the highest levels of ZnO and TiO_2 components.

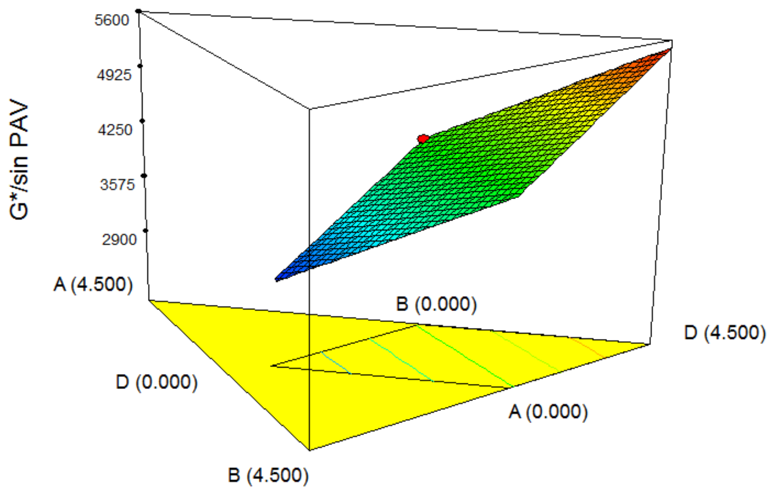

Fig. 7. 3D plot representing the influences of A= TiO_2, B = ZnO, and D = EVA variables on G^*/sin PAV

Conclusion

The methodology of Mixture Design a, type D-optimal was employed in the current work, and the values of SBS, ZnO, TiO_2, and EVA were considered the independent variables. The dependent or response variables followed as G*/sin OB, G*/sin RTFO, G*/sin PAV, RV, PEN, soft, ductility, m-value, and stiffness. Empirical data of the penetration degree, softening point, and ductility, conducted on the basic bitumen without any additives, were 89, 49 °C, and 137, respectively. The effects of independent variables were investigated on the response variables using the mathematic models and the optimized compositions. The maximum softening was detected at the highest EVA, and the minimum softening was observed at the largest ZnO and TiO_2. The SBS, ZnO, TiO_2, and EVA components elevated the ductility, and the largest positive effect belonged to the SBS constituent. The SBS and EVA variables positively elevated the G^*/sin OB response, in which the highest positive coefficient belonged to the EVA component.

In contrast, the ZnO and TiO_2 variables negatively decreased the G^*/sin OB response, in which the largest negative coefficient belonged to the ZnO constituent. The maximum G^*/sin PAV value was attained at the highest level of EVA, and the corresponding minimum value was detected at the highest levels of ZnO and TiO_2 components. The manipulated samples possessed a penetration range of 48–62 (1/10 mm). Softening point also ranged in 59–71 °C. Dynamic shear rheometric (DSR) data for the aged bitumens within short-term periods plummeted from 52 to 76 °C for all samples.

References

[1] Loeber L, Muller G, Morel J, Sutton O. Bitumen in colloid science: a chemical, structural and rheological approach. Fuel. 1998 Oct 1;77(13):1443-50.

[2] Lesueur D. The colloidal structure of bitumen: Consequences on the rheology and on the mechanisms of bitumen modification. Advances in colloid and interface science. 2009 Jan 30;145(1-2):42-82.

[3] Morian N, Hajj EY, Glover CJ, Sebaaly PE. Oxidative aging of asphalt binders in hot-mix asphalt mixtures. Transportation research record. 2011 Jan;2207(1):107-16.

[4] Dehouche N, Kaci M, Mokhtar KA. Influence of thermo-oxidative aging on chemical composition and physical properties of polymer modified bitumens. Construction and Building Materials. 2012 Jan 1;26(1):350-6.

[5] Mouillet V, Farcas F, Besson S. Ageing by UV radiation of an elastomer modified bitumen. Fuel. 2008 Sep 1;87(12):2408-19.

[6] Wu S, Pang L, Liu G, Zhu J. Laboratory study on ultraviolet radiation aging of bitumen. Journal of Materials in Civil Engineering. 2010 Aug;22(8):767-72.

[7] Liu YH, Fan YH, Zhang CY. Petroleum Asphalt, Petroleum Industry Press. Beijing, 1984.

[8] Apeagyei AK. Laboratory evaluation of antioxidants for asphalt binders. Construction and Building Materials. 2011 Jan 1;25(1):47-53.

[9] Cong P, Wang J, Li K, Chen S. Physical and rheological properties of asphalt binders containing various antiaging agents. Fuel. 2012 Jul 1;97:678-84.

[10] Yamaguchi K, Sasaki I, Nishizaki I, Meiarashi S, Moriyoshi A. Effects of film thickness, wavelength, and carbon black on photodegradation of asphalt. Journal of the Japan Petroleum Institute. 2005;48(3):150-5.

[11] Feng ZG, Yu JY, Kuang DL. The physical properties and photostability of bitumen with different ultraviolet absorbers. Petroleum Science and Technology. 2013 Jan 15;31(2):113-20.

[12] Yu JY, Feng PC, Zhang HL, Wu SP. Effect of organo-montmorillonite on aging properties of asphalt. Construction and Building Materials. 2009 Jul 1;23(7):2636-40.

[13] Mahdi LM, Muniandy R, Yunus RB, Hasham S, Aburkaba E. Effect of short term aging on organic montmorillonite nanoclay modified asphalt. Indian Journal of Science and Technology. 2013 Nov;6(10):5434-42.

[14] Zhang H, Yu J, Kuang D. Effect of expanded vermiculite on aging properties of bitumen. Construction and Building Materials. 2012 Jan 1;26(1):244-8.

[15] Zhang H, Shi C, Han J, Yu J. Effect of organic layered silicates on flame retardancy and aging properties of bitumen. Construction and Building Materials. 2013 Mar 1;40:1151-5.

[16] Zhang H, Zhu C, Yu J, Shi C, Zhang D. Influence of surface modification on physical and ultraviolet aging resistance of bitumen containing inorganic nanoparticles. Construction and Building Materials. 2015 Nov 15;98:735-40.

[17] Fini EH, Hajikarimi P, Rahi M, Moghadas Nejad F. Physiochemical, rheological, and oxidative aging characteristics of asphalt binder in the presence of mesoporous silica nanoparticles. Journal of Materials in Civil Engineering. 2016 Feb 1;28(2):04015133.

[18] Zhang HB, Zhang HL, Ke NX, Huang JH, Zhu CZ. The effect of different nanomaterials on the long-term aging properties of bitumen. Petroleum Science and Technology. 2015 Feb 16;33(4):388-96.

[19] Zhang H, Zhu C, Yu J, Tan B, Shi C. Effect of nano-zinc oxide on ultraviolet aging properties of bitumen with 60/80 penetration grade. Materials and Structures. 2015 Oct;48(10):3249-57.

[20] Liu CH, Zhang HL, Li S, Zhu CZ. The effect of surface-modified nano-titania on the ultraviolet aging properties of bitumen. Petroleum science and technology. 2014 Dec 17;32(24):2995-3001.

[21] Zhu C, Zhang H, Shi C, Li S. Effect of nano-zinc oxide and organic expanded vermiculite on rheological properties of different bitumens before and after aging. Construction and Building Materials. 2017 Aug 15;146:30-7.

[22] Porto M, Caputo P, Loise V, Eskandarsefat S, Teltayev B, Oliviero Rossi C. Bitumen and bitumen modification: A review on latest advances. Applied Sciences. 2019 Jan;9(4):742.

[23] Airey GD. Rheological properties of styrene butadiene styrene polymer modified road bitumens. Fuel. 2003 Oct 1;82(14):1709-19.

[24] Aglan H, Othman A, Figueroa L, Rollings R. Effect of styrene-butadiene-styrene block copolymer on fatigue crack propagation behavior of asphalt concrete mixtures. Transportation research record. 1993:178.

[25] Khattak MJ, Baladi GY. Engineering properties of polymer-modified asphalt mixtures. Transportation Research Record, 1998; 1638(1):12-22.

[26] Zhang W, Jia Z, Zhang Y, Hu K, Ding L, Wang F. The effect of direct-to-plant styrene-butadiene-styrene block copolymer components on bitumen modification. Polymers. 2019 Jan;11(1):140.

[27] Jasso M, Bakos D, MacLeod D, Zanzotto L. Preparation and properties of conventional asphalt modified by physical mixtures of linear SBS and montmorillonite clay. Construction and Building Materials. 2013 Jan 1;38:759-65.

[28] Zhu J, Birgisson B, Kringos N. Polymer modification of bitumen: Advances and challenges. European Polymer Journal. 2014 May 1;54:18-38.

[29] Tanzadeh J, Vahedi F, Kheiry PT, Tanzadeh R. Laboratory study on the effect of nano TiO2 on rutting performance of asphalt pavements. InAdvanced materials research 2013 (Vol. 622, pp. 990-994). Trans Tech Publications Ltd.

[30] Jahromi SG, Andalibizade B, Vossough S. Engineering properties of nanoclay modified asphalt concrete mixtures. Arabian Journal for Science & Engineering (Springer Science & Business Media BV). 2010 Apr 1;35.

[31] Golestani B, Nejad FM, Galooyak SS. Performance evaluation of linear and nonlinear nanocomposite modified asphalts. Construction and Building Materials. 2012 Oct 1;35:197-203.

[32] Van De Ven MF, Molenaar AA, Besamusca J, Noordergraaf J. Nanotechnology for binders of asphalt mixtures. InProceedings of the 4th Eurasphalt and Eurobitume Congress Held May 2008, Copenhagen, Denmark 2008.

[33] Ghasemi M, Marandi SM, Tahmooresi M, Kamali J, Taherzade R. Modification of stone matrix asphalt with nano-SiO2. Journal of Basic and Applied Scientific Research. 2012;2(2):1338-44.

[34] Khodadadi A, Kokabi M. Effect of Nanoclay on Long-Term Behavior of asphalt concrete pavement. In2st Congress of Nanomaterials, University of Kashan, Iran 2007.

[35] Shafabakhsh GH, Mirabdolazimi SM, Sadeghnejad M. Evaluation the effect of nano-TiO2 on the rutting and fatigue behavior of asphalt mixtures. Construction and Building Materials. 2014 Mar 15;54:566-71.

[36] Wang H, Liu X, Zhang H, Apostolidis P, Erkens S, Skarpas A. Micromechanical modelling of complex shear modulus of crumb rubber modified bitumen. Materials & Design. 2020 Mar 1;188:108467.

[37] Daryaee D, Ameri M, Mansourkhaki A. Utilizing of waste polymer modified bitumen in combination with rejuvenator in high reclaimed asphalt pavement mixtures. Construction and Building Materials. 2020 Feb 28;235:117516.

[38] Xing C, Liu L, Sheng J. A new progressed mastic aging method and effect of fillers on SBS modified bitumen aging. Construction and Building Materials. 2020 Mar 30;238:117732.

[39] Hussein AA, Putra Jaya R, Yaacob H, Abdul Hassan N, Oleiwi Aletba SR, Huseien GF, Shaffie E, Mohd Hasan MR. Physical, chemical and morphology characterisation of nano ceramic powder as bitumen modification. International Journal of Pavement Engineering. 2021 Jun 7;22(7):858-71.

How to cite: Karimian F, Beygi-Khosrowshahi Y. Physical/Rheological Characteristics of Bitumen Modified by SBS, ZnO, TiO_2 and EVA Precursors. Journal of Chemical and Petroleum Engineering. 2021; 55(2): 189-202.